journal

J. Am. Ceram. Soc., **86** [2] 257–65 (2003)

Reel-to-Reel Continuous Chemical Solution Deposition of Epitaxial Gd_2O_3 Buffer Layers on Biaxially Textured Metal Tapes for the Fabrication of $YBa_2Cu_3O_{7-\delta}$ Coated Conductors

Tolga Aytug,[†,‡] Mariappan P. Paranthaman,[*,†] Byeongwon W. Kang,[§] David B. Beach,[†] Srivatsan Sathyamurthy,[†] Eliot D. Specht,[§] Dominic F. Lee,[*,§] Roeland Feenstra,[‡] Amit Goyal,[*,§] Donald M. Kroeger,[§] Keith J. Leonard,[§] Patrick M. Martin,[§] and David K. Christen[*,‡]

Chemical Sciences Division, Solid State Division, and Metals and Ceramics Divison, Oak Ridge National Laboratory, Oak Ridge, Tennessee 37831

A nonvacuum reel-to-reel dip-coating system has been used to continuously fabricate epitaxial Gd_2O_3 buffer layers on mechanically strengthened, biaxially textured Ni–(3 at.% W–1.7 at.% Fe), defined as Ni-alloy, metal tapes. Because of its significance as a seed layer, optimum processing conditions (postannealing speed and temperature) of Gd_2O_3 buffer layers have been studied. Highly textured films were obtained under reducing (96% Ar + 4% H_2) atmosphere at temperatures between 1100° and 1150°C; postannealing speed did not significantly affect the crystalline quality of the Gd_2O_3. Scanning electron microscopy revealed a continuous, dense, and crack-free surface morphology for these dip-coated buffers. The Gd_2O_3 layer thickness led to pronounced differences in the growth characteristics of the subsequent YSZ and CeO_2 layers deposited by rf-magnetron sputtering. Epitaxial YBCO films grown by pulsed laser deposition on the short prototype CeO_2/YSZ/Gd_2O_3/Ni–(3 at.% W–1.7 at.% Fe) conductors yielded self-field critical current densities (J_c) as high as 1.2×10^6 A/cm^2 at 77 K. Pure Ni tapes were used to assess the viability of dip-coated buffers for long length coated conductor fabrication. The YBCO films, grown on 80 cm long and 1 cm wide CeO_2/YSZ/Gd_2O_3 buffered Ni tapes by the industrially scalable *ex situ* BaF_2 precursor process, exhibited end-to-end self-field J_c values of 6.25×10^5 A/cm^2 at 77 K. These results demonstrate the reproducible epitaxy of solution-derived seed layers on pure Ni and Ni-alloy tapes as well as underscore the viability of solution approaches for the production of long length YBCO-based coated conductors.

I. Introduction

RECENTLY, scalable techniques for achieving long lengths of biaxially textured buffer layers and superconductors on Ni or Ni-alloy substrates have been proposed. One of the approaches uses the concept of rolling-assisted biaxially textured substrates (RABiTS).[1,2] This technique employs thermomechanical processing to obtain sharp biaxially textured metal tapes, which can be produced over long lengths. The primary issue for the successful development of coated conductors for high-temperature superconducting (HTS) wire applications is to chemically isolate the HTS film from the metal substrate, preventing diffusion of Ni into the superconductor during high-temperature processing, and also provide an epitaxial template for growth of the HTS coating. Various combinations of oxide buffer layers have been tried on metallic substrates for the development of HTS-coated conductors.[1–14] The most successful tape architecture has been the combination of CeO_2 and yttria-stabilized zirconia (YSZ), yielding $YBa_2Cu_3O_{7-\delta}$ (YBCO) films with high critical current densities (J_c) exceeding 10^6 A/cm^2 (77 K, 0 T).[2,8,10–13] Fabrication of these buffer layers is generally conducted by vapor deposition processes such as electron beam evaporation (e-beam), pulsed laser deposition (PLD), or magnetron sputtering.[1–13] A major challenge in using any of these buffer-deposition techniques is prevention of unfavorably oriented NiO on the Ni surface.[2,10–13,15] This requirement is difficult in principle since the growth of oxide films generally requires elevated temperatures and oxidizing environment. Another issue of concern has been the formation of cracks in the base CeO_2 layer at thicknesses greater than a few hundred angstroms;[10,16,17] it is well understood that integrity of a seed buffer layer is crucial for reproducible epitaxial growth of subsequent oxide buffer and HTS layers.

For the commercial development of a practical superconducting wire technology, more adaptive and easily scalable processing techniques are highly required. Nonvacuum chemical solution based processes,[18–28] such as sol–gel and metal-organic decomposition (MOD), offer many desirable aspects, such as precise control of metal oxide precursor stoichiometry and composition, mechanical simplicity, and low cost. Recently, it has been reported that various RE_2O_3 (rare-earth (RE) = Gd, Yb, and Eu) and $RE_2Zr_2O_7$ (RE = La and Nd) oxide films can grow epitaxially on textured Ni substrates by using solution-based methods.[23–25,28] While short segments of sol–gel seeded Ni substrates with sputtered CeO_2/YSZ overlayers have yielded YBCO with J_c in the range of 0.4×10^6–1.1×10^6 A/cm^2 at 77 K,[23–25,28] long lengths of high-J_c YBCO coatings on solution seed buffer layers have not yet been produced.

Much of the work reported using the RABiTS technique has used high-purity Ni (99.99%) as the texture material. However, the low mechanical strength and ferromagnetism of pure Ni present significant challenges in long length manufacturing and hinders its usage in applications where AC losses are an issue. Therefore, it is desirable to work with textured alloy substrates that are much stronger and nonmagnetic, or have reduced magnetism. Recently, the successful texturing of Ni strengthened with small additions (3–5 at.%) of W and (1.7 at.%) Fe has been reported.[29,30] These substrates, typically 50 μm thick, accommodate similar annealing

B. A. Tuttle—contributing editor

Manuscript No. 187380. Received October 23, 2001; approved November 26, 2002.

This work was supported by the U.S. Department of Energy, Division of Materials Sciences, Office of Science, Office of Power Technologies—Superconductivity Program, Office of Energy Efficiency and Renewable Energy. The research was performed at the Oak Ridge National Laboratory, managed by U.T.-Battelle, LLC, for the U.S. Department of Energy under Contract No. DE-AC05-00OR22725. Acknowledgments also extended to Oak Ridge Associated Universities for their support.

[*]Member, American Ceramic Society.
[†]Chemical Sciences Division.
[‡]Solid State Division.
[§]Metals and Ceramics Division.

conditions and show comparable grain sizes to those of pure Ni. After recrystallization, however, they exhibit yield strengths (YS) of 143 and 154 MPa at 0.02% and 0.2% strain, respectively, which are much higher than those of pure Ni (YS = 40 and 58 MPa, respectively).[29] In addition, the saturation magnetization, M, of a Ni–(3 at.% W–1.7 at.% Fe), [Ni-alloy], (M = 40 G·cm^3/g) was found to be significantly lower than that of pure Ni (M = 57.5 G·cm^3/g at T = 0 K). Development of oxide buffer layers and HTS coatings by both vacuum and nonvacuum processes on these alloys has just begun.[28,30,31] Recently, high-quality YBCO films with J_c (self-field, 77 K) values of 1.9×10^6 A/cm^2 have been demonstrated on such substrates where the oxide buffer layers have been grown by all-vacuum processes.[31] In addition to vacuum-based techniques, oxide buffer layers have also been grown directly on Ni-alloy tapes by nonvacuum solution-based methods. However, despite a good crystalline structure, to date there have been no reports on the growth of high-J_c YBCO films on these sol–gel buffered alloy tapes.

In this paper, first we report the epitaxial growth and property characterizations of sol–gel processed, reel-to-reel dip-coated Gd_2O_3 seed buffer layers on textured Ni-alloy substrates. Effects of processing parameters on seed-layer quality and carbon retention were systematically explored. Second, as a proof of principle, we present the growth of high- quality YBCO coatings on short segments of these Gd_2O_3/Ni–(3 at.% W–1.7 at.% Fe) tapes with sputtered CeO_2/YSZ cap buffer layers. Third, we extend short sample studies to demonstrate for the first time the continuous fabrication of high-J_c HTS coatings in long lengths on pure Ni tapes that have solution processed seed layers. The electrical transport properties, measured over lengths (100 cm) of YBCO films grown using the *ex situ* BaF_2 precursor process, are also reported.

II. Experimental Procedure

(1) Preparation of Biaxially Textured Ni and Ni-Alloy Substrates

Biaxially textured Ni (99.99%) and Ni–(3 at.% W–1.7 at.% Fe) substrates were obtained by progressive cold rolling of polycrystalline, randomly oriented Ni and Ni-alloy bars to a total deformation of 95%–98%. After mechanical deformation, 50 μm thick and 1 cm wide substrates were first cleaned with isopropyl alcohol in a reel-to-reel ultrasonic cleaning unit, and then annealed at 1100°C (for pure Ni) and 1250°C (for Ni-alloy) for 1 h in a reducing, forming gas (96% Ar + 4% H_2) atmosphere. The procedure yields the desired {100}⟨100⟩ cube texture to typical levels of 6–8° FWHM.

(2) Preparation of Gd_2O_3 Solution and Coating Procedure

A 2-methoxyethanol solution of gadolinium methoxyethoxide/acetate, prepared by an alkoxide sol–gel synthesis route, was used to coat the Ni and Ni-alloy tapes. The solution preparation was conducted under Ar gas atmosphere using a Schlenck-type apparatus. To avoid premature hydrolysis, which can induce precipitation, the as-received gadolinium acetate powder was first purified by dissolving in a mixture of water and acetic acid at a ratio of 3:1, filtered, and then evaporated to dryness in an oven maintained at 150°C for overnight to remove absorbed moisture. Then the purified gadolinium acetate of about 3.34 g was dissolved in 40 mL of 2-methoxyethanol in a 250 mL round-bottomed flask. The flask was refluxed for 1 h with excess 2-methoxyethanol to exchange the acetic acid ligand with the methoxyethoxide ligand. The final volume was adjusted to 40 mL to produce a 0.5M Gd_2O_3 precursor solution.

In a reel-to-reel dip-coating unit, tapes with dimensions of 10 cm in length and 1 cm in width were coated to determine the optimum processing parameters of Gd_2O_3 seed layers on Ni-alloy. The textured tapes were continuously pulled through the Gd_2O_3 precursor solution at a constant speed in the range of 20–300 cm/h. These double-sided, dip-coated tapes were then transported, in a flowing forming gas atmosphere, through a preheated furnace at various temperatures (T_{an}) ranging from 1050° to 1250°C. For this processing, different tape transport speeds (S_{an}) in the range of 5 to 30 cm/h were investigated, resulting in heating rates of 6° to 40°C/min, respectively. The rate is limited by the length of the uniform hot zone for the present furnace, which spans ~10 cm. After the growth conditions of Gd_2O_3 on Ni-alloys were optimized based on structural and morphologic characterizations, the same parameters were used for the growth on Ni tapes. In fact, from detailed studies (not shown here) the growth conditions of Gd_2O_3 on both substrates are found to be similar.

(3) Preparation of YBCO Test Structures

Sputtering by the rf-magnetron technique was used to deposit both YSZ and CeO_2 overlayers on short segments of the dip-coated substrates, yielding the buffer-layer sequence CeO_2/YSZ/Gd_2O_3/Ni–(3 at.% W–1.7 at.% Fe). Oxide sputtering targets were 2 in. in diameter and the system base pressure was 1×10^{-6} torr. Samples were attached onto a heated substrate block assembly by clipping at both ends, in an on-axis sputtering geometry. Sputtering conditions for both oxides consist of a mixture of 10 mtorr of forming gas and 2×10^{-6} torr of H_2O, and a substrate temperature of 780°C. Typical film thicknesses for these YSZ and CeO_2 layers were around 200 and 20 nm, respectively.

To assess the quality of the CeO_2/YSZ/Gd_2O_3/Ni-alloy multilayer structure, YBCO films were deposited by pulsed laser deposition (PLD), using a XeCl excimer laser system, operated with energy density of ≈4 J/cm^2. Details of the experimental conditions were reported elsewhere.[7–9] Typical YBCO film thicknesses were 200 nm.

(4) Characterization Techniques

X-ray diffraction analysis was used to analyze phase, structure, and texture (i.e., the orientation relationship of the grains relative to the substrate material geometry) of the buffer layers as well as the YBCO coatings deposited on short samples. A Philips Model XRG3100 diffractometer with Cu$K\alpha$ radiation was used to record powder diffraction patterns. Texture analysis was achieved using a Rigaku rotating anode X-ray generator with a graphite incident-beam monochromator selecting Cu$K\alpha$ with slits defining 2 mm × 2 mm beam. Pole figures were collected with a 4-circle diffractometer. The out-of-plane (ω-rocking curve scans) alignment of the films was measured by rocking the desired (00l) planes about an axis perpendicular to the scattering plane (ω-axis) and the in-plane (ϕ-scan) alignments were measured by rotating the desired (hkl) planes around the normal to the sample plane. Peak width FWHM values were determined by least-squares fitting to Gaussian line shapes. The texture of long-length samples was measured with a larger diffractometer (Model 4-circle, Huber) to accommodate a reel-to-reel translation stage. Data were obtained as a function of position by continuously measuring out-of-plane (ω-rocking curve scan) and in-plane (ϕ-scan) alignments, while translating the sample. Microstructural investigations were conducted using a Hitachi S-4100 high-resolution field emission type scanning electron microscope (HRSEM). The thickness of the buffer and superconducting layers was determined by Rutherford backscattering spectroscopy (RBS). In addition, ion spectroscopy techniques were used to determine the carbon content of the dip-coated buffers, by using a resonance for the 1.73 MeV H^+ ions at near normal incidence. A standard four-point contact technique was applied to measure the superconducting critical temperature (T_c) and J_c of the YBCO films. For short samples, the distance between voltage contacts was 4 mm and the values of J_c were assigned at a 1 μV/cm criterion. Electrical contacts of silver were deposited onto the samples using dc-magnetron sputtering followed by an O_2 annealing in 1 atm for 30 min at 500°C.

III. Results and Discussion

(1) Growth of Gd_2O_3 Seed Layers on Biaxially Textured Ni-Alloy Substrates

Figure 1 shows the XRD θ–2θ spectrum for a series of dip-coated Gd_2O_3 seed layers processed at various temperatures

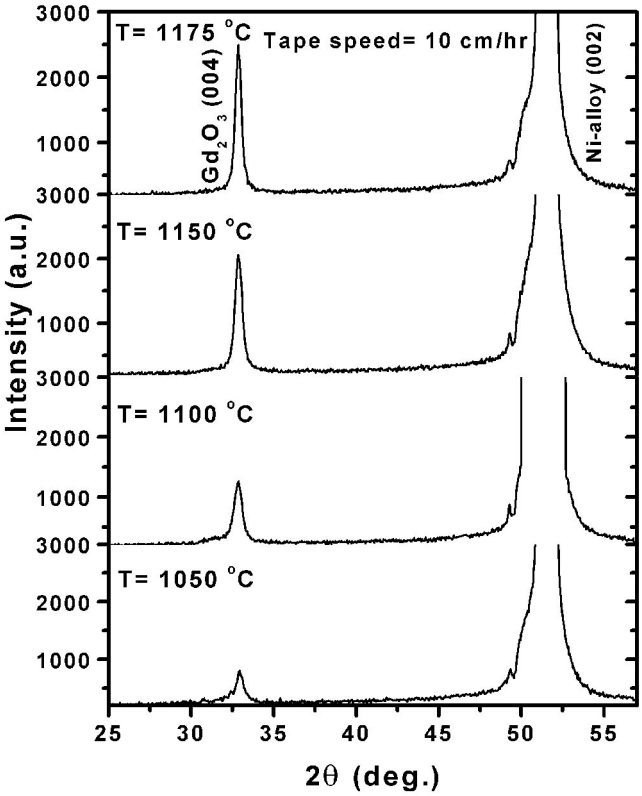

Fig. 1. XRD θ–2θ patterns of dip-coated Gd_2O_3 films grown on biaxially textured Ni–(3 at.% W–1.7 at.% Fe) substrates at various annealing temperatures.

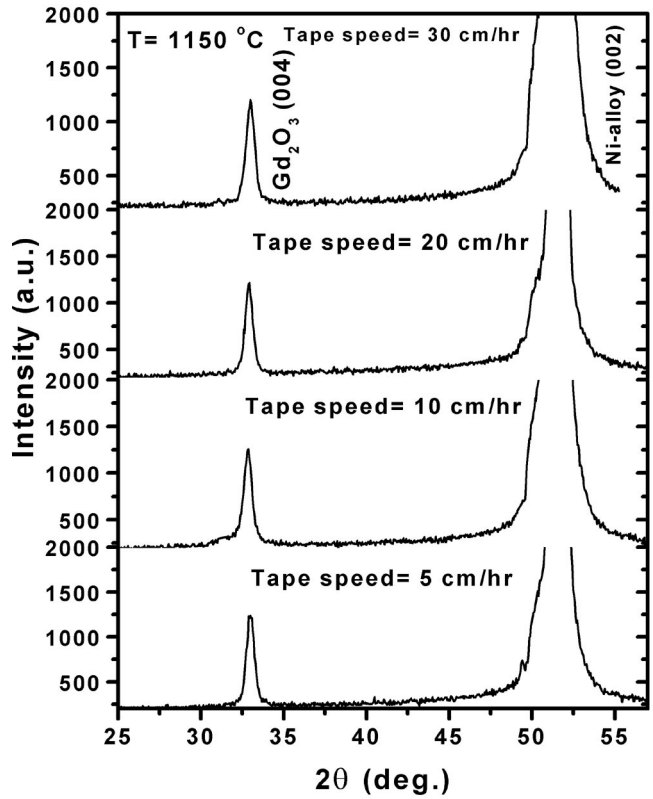

Fig. 2. XRD θ–2θ patterns of dip-coated Gd_2O_3 films grown on biaxially textured Ni–(3 at.% W–1.7 at.% Fe) substrates at 1150°C, for various annealing speeds.

ranging from 1050° to 1170°C at a fixed S_{an} of 10 cm/h. At $T_{dep} \leq 1100$°C, broad and relatively low intensity (00*l*) Gd_2O_3 reflections are observed as evidence of inhomogeneity or high structural defect density. For 1100°C $< T_{dep} <$ 1175°C, the (00*l*) peak intensities increase and the reflections sharpen, indicating substantial improvement in the crystalline quality of the films. Since dip-coated film thickness is directly proportional to the coating speed, which was kept constant for each individual sample, comparison of the relative Gd_2O_3 (00*l*) peak intensities reflects the crystalline quality of the films. At temperatures above 1200°C, however, the films showed extra Gd_2O_3 peaks reflections, which are indexed as belonging to Gd_2O_3 monoclinic phase components.[32,33] To investigate the influence of annealing speed on the crystalline quality of Gd_2O_3, a series of films were annealed at T_{an} = 1150°C in different S_{an} in the range of 5–30 cm/h. From the comparable (00*l*) θ–2θ peak intensities, shown in Fig. 2, it is apparent that S_{an} does not significantly affect the crystalline quality of the Gd_2O_3. The effect of T_{an} on the in-plane and the out-of-plane texture of Gd_2O_3 layers was also studied at a fixed S_{an} = 10 cm/h, and the results are shown in Figs. 3(a) and (b), respectively. Note that biaxially textured Ni-alloy substrates generally have slightly different in-plane and out-of-plane textures depending on the specific rolling and crystallization conditions. Thus, to make a direct and more quantitative comparison between the processing parameters and the crystalline quality of the grown films, the FWHM peak-width ratio relative to the underlying Ni-alloy is plotted as a function of T_{an}. Substantial improvement in the in-plane and out-of-plane alignment of the Gd_2O_3 layers is observed with an increase in temperature above 1050°C. Depositions at $T_{an} >$ 1100°C, however, did not significantly affect the epitaxial quality. Similarly the effect of S_{an} on the epitaxial growth of the films (for the same samples studied in Fig. 2) can be observed from the results of ω- and ϕ-scan peak-width ratios, as shown in Fig. 4, for a fixed T_{an} = 1150°C. While S_{an} does not have a remarkable influence on the in-plane alignment of the films, an increase in S_{an} over 20 cm/h has a negative effect on the out-of-plane texture, as evidenced by the gradual increase in the ω-scan FWHM ratios. Since the uniform hot-zone length is ~10 cm for the present furnace, the latter effect for higher S_{an} can be correlated with the decreased residence time in the effective hot-zone region. On the other hand, the in-plane alignment is likely governed by the crystallographic texture of the underlying substrate. Hence, the combined observations of Figs. 1–4 suggest that the optimal range for epitaxial growth of Gd_2O_3 on Ni–(3 at.% W–1.7 at.% Fe) should be a T_{an} of 1100° to 1175°C and $S_{an} <$ 30 cm/h.

The epitaxial quality of the Gd_2O_3 films was examined by XRD pole figure analysis. The logarithmic-scale (222) pole figures for two films processed at T_{an} = 1150°C and S_{an} = 20 cm/h, having thin (25 nm) and thick (73 nm) Gd_2O_3 layers, are shown in Figs. 5(a) and (b), respectively. The data for both films indicate single-domain epitaxy, with the Gd_2O_3[001]//substrate[001] and Gd_2O_3[110]//substrate[100]. This result is important, since any other orientational domains could lead to the potential disruption of current flow by high-angle grain boundaries in the HTS layer.

For implementation of nonvacuum dip-coated Gd_2O_3 seed layers into long-length wire manufacturing, it is important to grow dense and crack-free layers with minimum carbon contamination. Resonant RBS has been used to analyze the carbon levels (number of carbon atoms/number of gadolinium atoms) in several Gd_2O_3 samples, with an interest on the correlation with respect to T_{an} and S_{an}. The results are summarized in Table I. The slight variations in thickness for the same coating speed are due to differences in the solution viscosity. While we observe no strong dependence of carbon content on either T_{an} or S_{an}, the overall carbon levels are significant (≈0.4–0.6 carbon/gadolinium atom). These levels, however, do not adversely affect the surface morphology of the thinner buffers, as shown in the following. Plan-view HRSEM micrographs of the surface morphology for 25 and 73 nm thick Gd_2O_3 films fabricated on biaxially textured Ni-alloy substrates are presented in Figs. 6(a) and (b), respectively. While each sample exhibits a continuous, crack-free, and dense surface morphology, significant surface roughening develops for the thicker coatings (Fig.

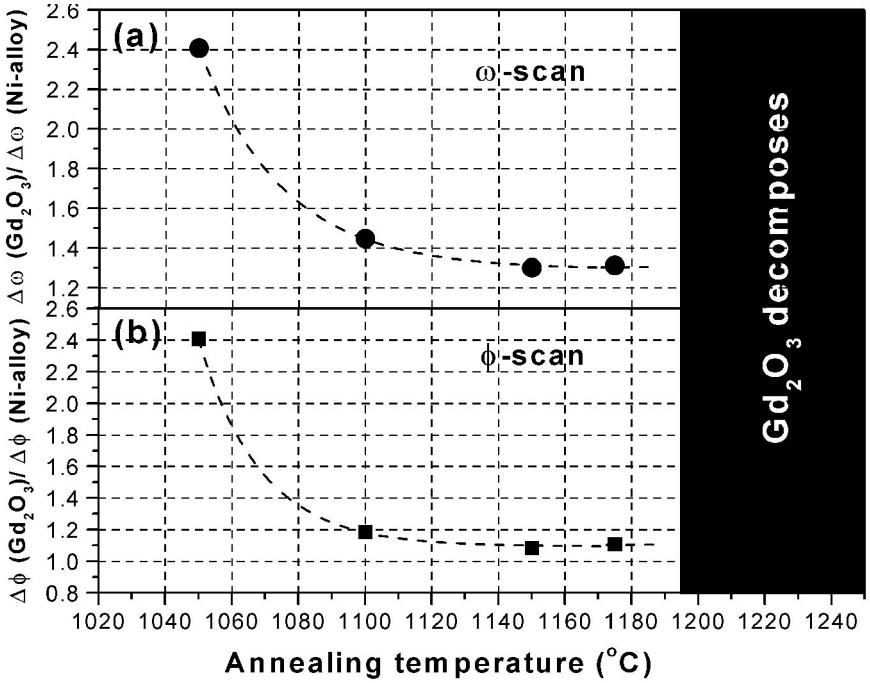

Fig. 3. Dependence of the normalized XRD FWHM peak widths, quantifying the crystallinity of Gd_2O_3 films as a function of postannealing temperature: (a) the out-of-plane distribution width $\Delta\omega$; (b) the in-plane distribution width $\Delta\phi$. The lines serve as a visual guide.

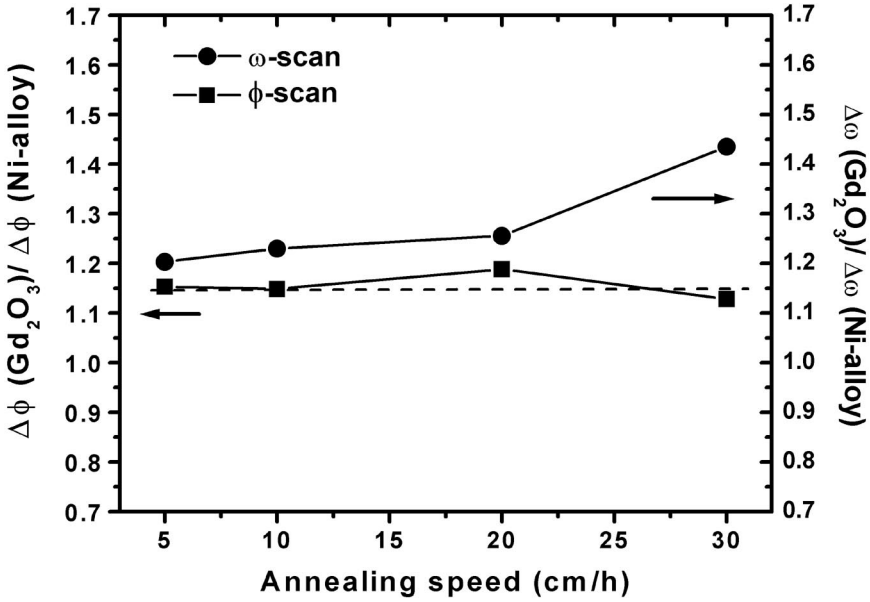

Fig. 4. Effect of postannealing speed on the FWHM ratios of ω-rocking curves and ϕ-scans for Gd_2O_3 films on Ni–(3 at.% W–1.7 at.% Fe) tapes, fabricated at 1150°C. The dashed line serves as a visual guide.

6(b)). On the other hand, thinner coatings (25 nm) exhibit extremely smooth and featureless surface microstructure (Fig. 6(a)), with an rms roughness of ~3 nm as determined by atomic force microscopy measurements. Such surface morphology should best serve the goal of obtaining high-quality YBCO coatings, despite the internal carbon content of the Gd_2O_3. The effects of Gd_2O_3 seed layer thickness on the growth characteristics of subsequent oxide buffer layers are discussed in the following section.

(2) Structural and Superconducting Property Characterizations of YBCO/CeO_2/YSZ/Gd_2O_3/Ni-Alloy Multilayer Structure

After optimizing the fabrication process for dip-coated Gd_2O_3 films on Ni-alloys, we have first deposited YSZ and CeO_2 overlayers by rf-magnetron sputtering, and then investigated the quality of this solution seeded CeO_2/YSZ/Gd_2O_3 buffer layer structure by depositing YBCO films. In this architecture the YSZ buffer layer acts as a Ni diffusion barrier and the CeO_2 layer ensures a better lattice match with YBCO. Figures 7(a) and (b) show the results of XRD θ–2θ scans for the CeO_2/YSZ bilayers deposited on Gd_2O_3/Ni-alloy substrates, where the Gd_2O_3 layer thickness is 25 and 73 nm, respectively. The data show that CeO_2/YSZ bilayers grown on thicker Gd_2O_3 layers have a polycrystalline nature (Fig. 7(b)), whereas films deposited on thinner seed layers exhibit excellent *c*-axis oriented growth (Fig. 7(a)). This growth behavior seems overwhelmingly governed by the surface morphology of the Gd_2O_3 films. It is known that surface roughness exacerbates adverse interfacial reaction between the

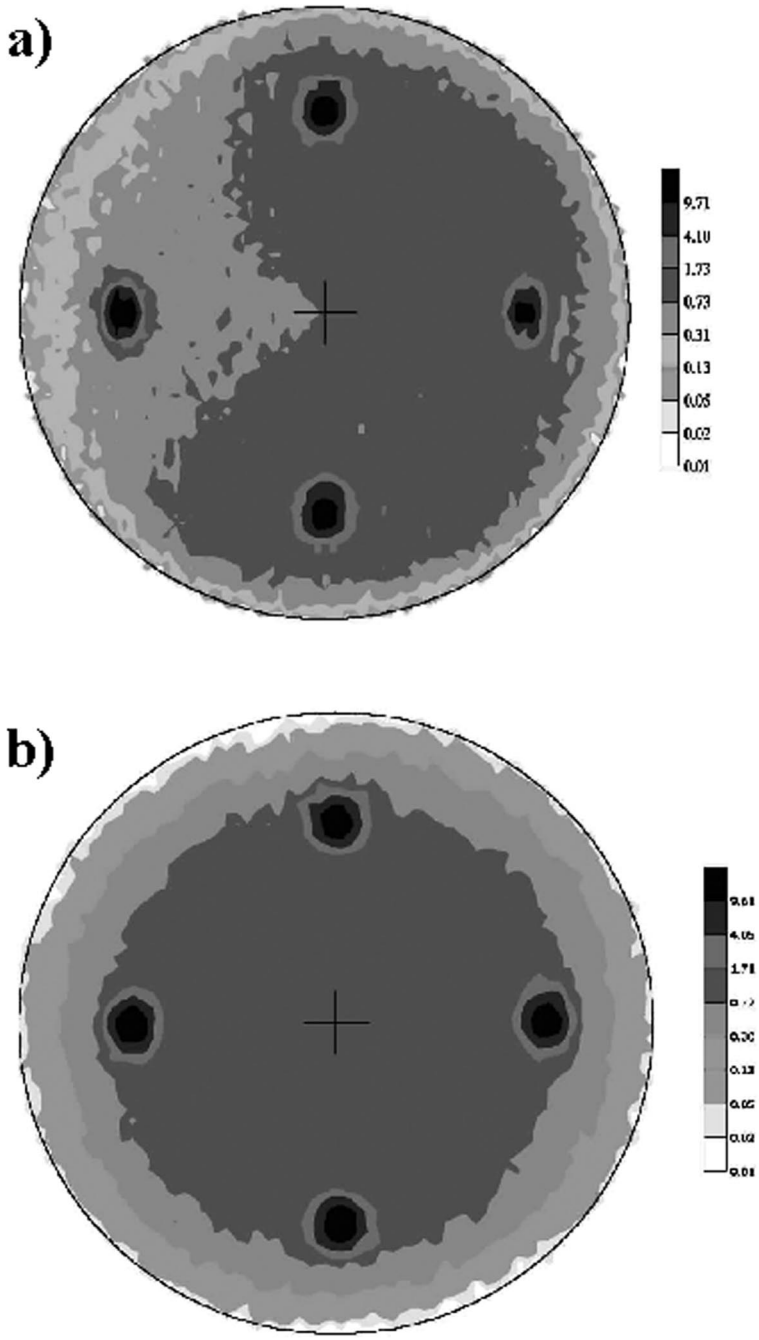

Fig. 5. The (222) logarithmic pole figure of (a) 25 nm and (b) 73 nm thick dip-coated Gd_2O_3 film processed on biaxially textured Ni–(3 at.% W–1.7 at.% Fe) at 1150°C with an annealing speed of 20 cm/h.

film and the substrate. Therefore, the relatively coarse surface morphology of thicker Gd_2O_3 films could contribute to polycrystalline growth behavior of the CeO_2/YSZ overlayers.

Following deposition of CeO_2/YSZ overlayers, suitability of the CeO_2/YSZ/Gd_2O_3/Ni-alloy structure was tested with the growth of YBCO films. A typical XRD θ–2θ scan is shown in Fig. 7(c), where the pattern indicates only (00*l*) reflections for the YBCO, demonstrating *c*-axis perpendicular to the substrate surface. After YBCO deposition, weak NiO impurity peaks are observed at 37° and 44°, implying minor oxidation of the metal substrate interface during the HTS processing step. However, this occurrence seems to have no adverse effect on the superconducting properties. The relative in-plane and out-of-plane textures between individual layers are documented in Figs. 8(a) and (b), respectively. The ω-rocking curve scans (Fig. 8(a)) obtained through the (002) peak reflections for Ni, YSZ, and CeO_2 (004), reflection for Gd_2O_3, and

Table I. Processing Conditions and the Resulting Carbon Contents of Several Dip-Coated Gd_2O_3 Films for a Series of Annealing Temperatures, Annealing Speeds, and Coating Speeds

Temperature (°C)	Coating speed (cm/h)	Annealing speed (cm/h)	Gd_2O_3 thickness (Å)	No. of carbon at. / No. of Gd at.
1050	300	10	730	0.59
1100	300	10	670	0.58
1150	300	10	710	0.37
1175	300	10	730	0.39
1150	20	5	185	0.55
1150	20	20	130	0.49
1150	20	30	250	0.41

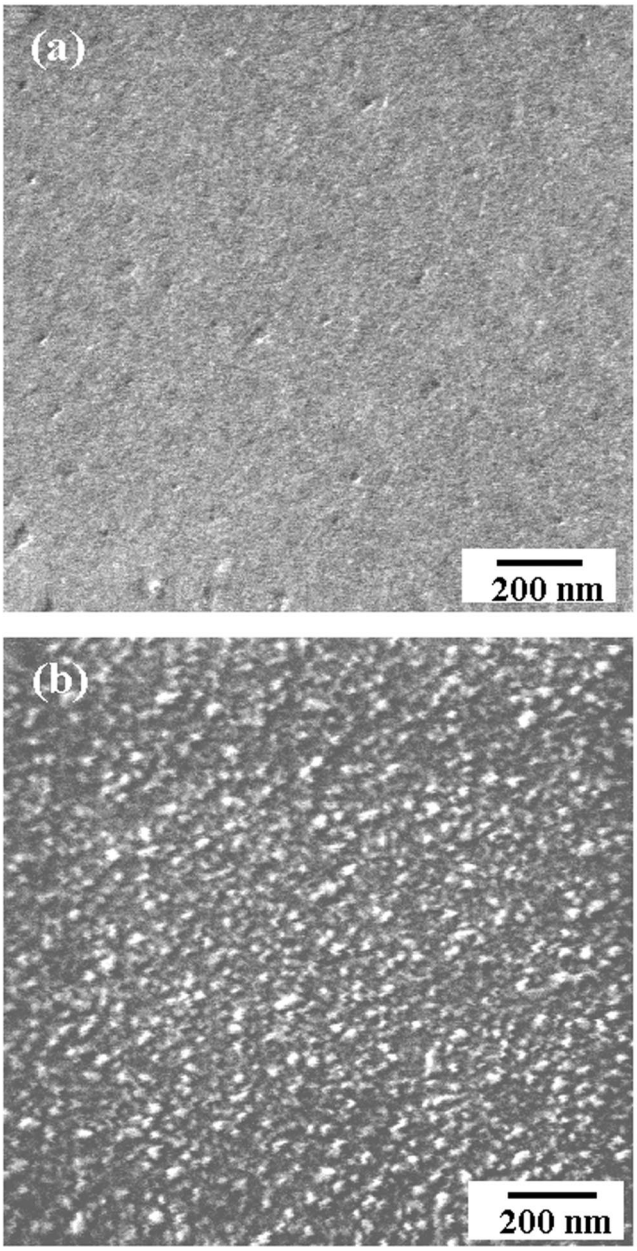

Fig. 6. High-resolution SEM micrographs for (a) 25 nm and (b) 73 nm sol–gel dip-coated Gd_2O_3 seed layers on (100) textured Ni–(3 at.% W–1.7 at.% Fe) substrates.

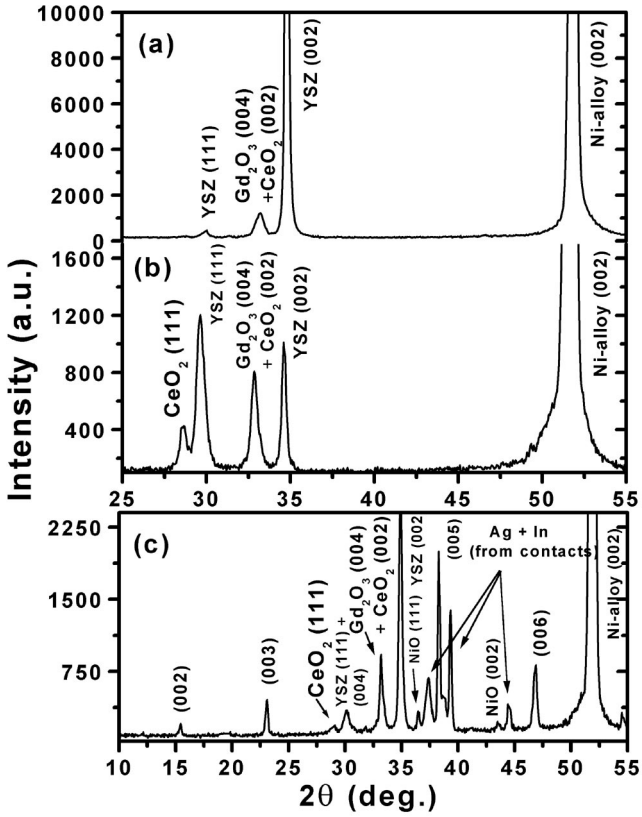

Fig. 7. XRD θ–2θ scans, of the CeO_2/YSZ bilayers on Gd_2O_3/Ni–(3 at.% W–1.7 at.% Fe) substrates, where the Gd_2O_3 layer thickness is about (a) 25 and (b) 73 nm. (c) A typical XRD θ–2θ spectrum for a YBCO film on the CeO_2/YSZ/Gd_2O_3(20 nm)/Ni–(3 at.% W–1.7 at.% Fe) multilayer structure. YBCO peaks are labeled by (00*l*) indexes.

the (006) reflection for YBCO, yield peak-width FWHM values (Δω) of 5.2°, 7.2°, 7.7°, 6.4°, and 5.8°, respectively, indicating good out-of-plane crystallographic alignment among the layers. In-plane textures of the individual layers for the same sample are illustrated in Fig. 8(b), where ϕ-scan data through the YBCO(103), CeO_2(111), YSZ(111), Gd_2O_3(222), and Ni(111) reflections reveal four equally spaced peaks, with similar in-plane FWHM values (Δϕ) of about 8–9°. These in-plane epitaxial orientations correspond to CeO_2, YSZ, and Gd_2O_3 basal planes that are rotated 45° relative to in-plane Ni-alloy substrate (100) axis, whereas the *a*-axis and *b*-axis of the YBCO are rotated 45° with respect to the top CeO_2 axes. The observed 45° rotations are anticipated according to the lattice match considerations between subsequent layers.

Since the qualifying test for any coated-conductor buffer-layer structure is compatibility with the deposition of high-quality, high-J_c YBCO coatings, electrical transport and superconducting property measurements were conducted on the same sample. Figure 9 compares the magnetic field (*H*//*c*-axis) dependence of J_c at 77 K with those of YBCO films grown on solution derived CeO_2/YSZ/Gd_2O_3(dip-coated)/Ni and on standard, all vacuum deposited, buffer layer RABiTS architecture of CeO_2/YSZ/CeO_2/Ni. The inset of this figure shows the superconducting transition region of the temperature-dependent resistivity, yielding a zero-resistance T_c = 90.5 K. The zero-field transport J_c of the YBCO/CeO_2/YSZ/Gd_2O_3/Ni-alloy sample is 1.2×10^6 A/cm^2 and it exhibits a high irreversibility field (H_{irr}) of 7 T. This J_c performance is comparable to that of epitaxial YBCO films on CeO_2/YSZ/Gd_2O_3(dip-coated) and all-vacuum CeO_2/YSZ/CeO_2 buffered biaxially textured Ni substrates. Thus, the microstructural requirements for high-J_c are imparted in YBCO through the CeO_2/YSZ/Gd_2O_3, including a near absence of weak-linked high-angle grain boundaries and an overall high degree of in- and out-of-plane alignment. The slight differences in high-field J_c behavior of the different samples arise from subtle variations in flux pinning properties, which can be associated with small changes in YBCO deposition conditions, composition, and substrate surface properties.

(3) Long-Length Fabrication of RABiTS Architecture Based on Dip-Coated Gd_2O_3/Ni Tapes

Having realized excellent structure and superconducting properties of YBCO films on short segments of CeO_2/YSZ capped, sol–gel synthesized Gd_2O_3 seed layers, we devoted our efforts to long-length implementation of the same architecture on Ni tapes. Figure 10 plots the XRD ω-rocking curve intensity distributions for the CeO_2(002) + Gd_2O_3(004) and YSZ(002) peak reflections taken along a 1 m length of CeO_2/YSZ/Gd_2O_3(dip-coated) buffered Ni tape. The tape was drawn through the solution at a rate of 80 cm/h, and the film was annealed in a preheated furnace at a speed of 20 cm/h at 1130°C. It should be mentioned that by reducing the concentration of Gd_2O_3 precursor solution from 0.5*M* to 0.25*M*, 80 cm/h coating speed results in a layer thickness of

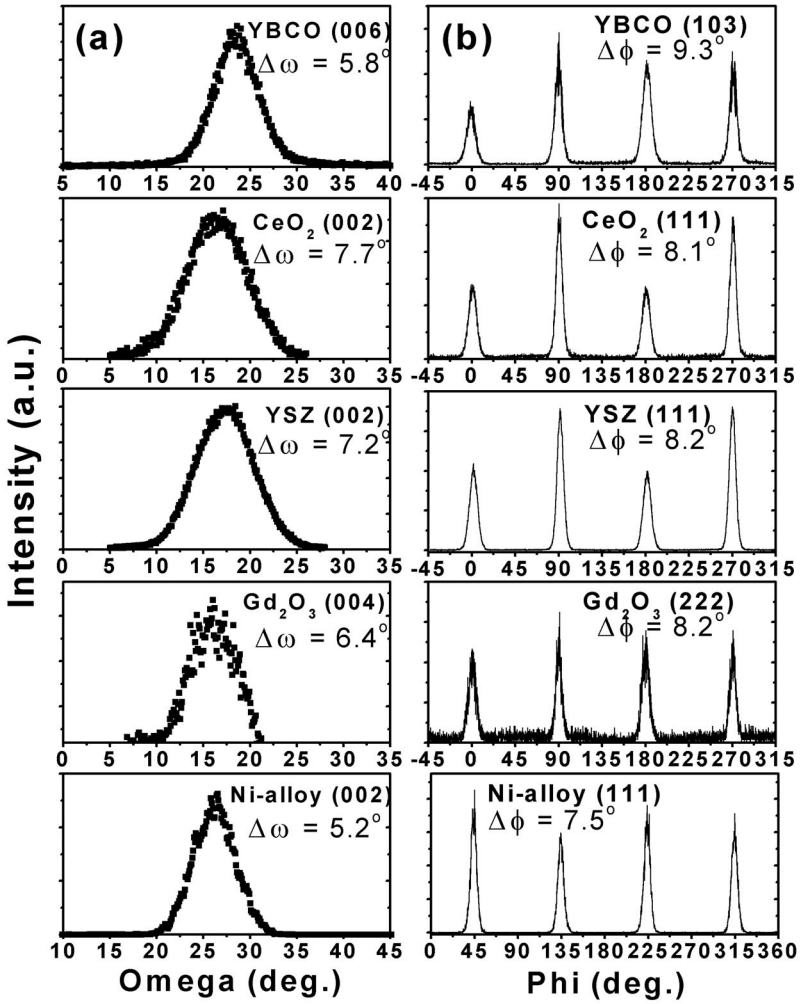

Fig. 8. XRD (a) out-of-plane (ω-scans) and (b) in-plane (ϕ-scans) texture for an epitaxial YBCO film (200 nm thick) on a $CeO_2/YSZ/Gd_2O_3$/Ni–(3 at.% W–1.7 at.% Fe) multilayer structure. The FWHM (Δω and Δϕ) for each scan are indicated.

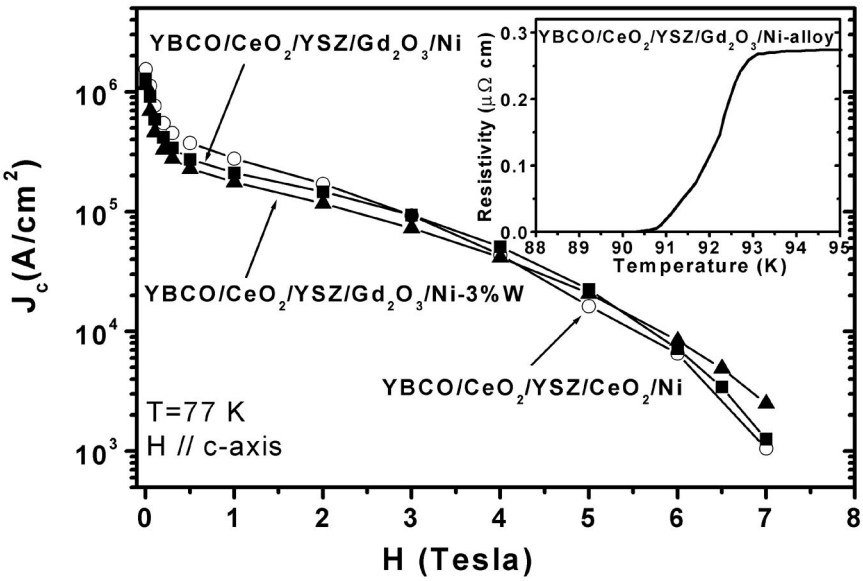

Fig. 9. Magnetic field dependence of J_c, measured at 77 K, for a YBCO film on the $CeO_2/YSZ/Gd_2O_3$/Ni–(3 at.% W–1.7 at.% Fe) multilayer structure. Also shown for comparison are J_c (H, 77 K) for the YBCO/$CeO_2/YSZ/Gd_2O_3$/Ni and YBCO/$CeO_2/YSZ/CeO_2$/Ni. The inset shows the resistive superconducting transition region of the present sample.

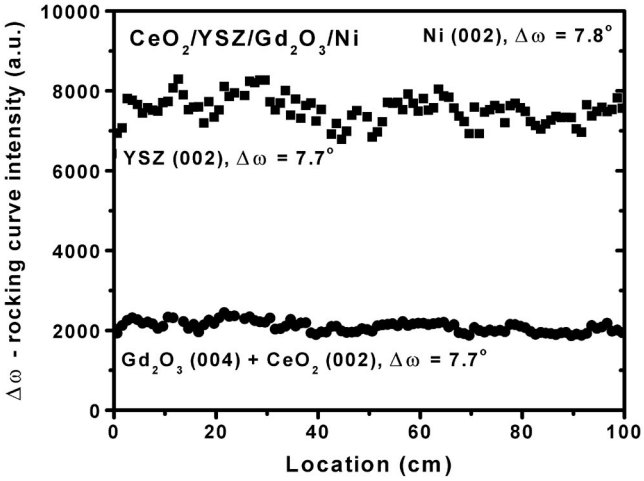

Fig. 10. XRD ω-rocking curve intensity distributions for the CeO_2(002) + Gd_2O_3(004) and the YSZ(002) peak reflections as a function of the length over a 1 m vacuum and nonvacuum processed $CeO_2/YSZ/Gd_2O_3$ buffer layers on biaxially textured Ni tape.

~20–25 nm. Uniform *c*-axis alignment among the buffer layers can be seen from this figure. Slight changes in the ω-rocking curve intensities are due to variations in the thickness of the buffer layers. Since the Bragg angles for the CeO_2(002) and Gd_2O_3(004) reflections are nearly coincident, it was not possible to distinguish them within the resolution of our XRD system. Similarly, excellent uniformity for the in-plane texture of the YSZ layer is evident from the plot (Fig. 11) of XRD ϕ-scan intensity distribution recorded from the YSZ(111) reflection along the tape length. The ω- and ϕ-scan FWHM values of 7.7° and 8.7° obtained for CeO_2–YSZ–Gd_2O_3 buffers and YSZ layer, respectively, are comparable to those of the Ni substrate ($\Delta\omega = 7.8°$, $\Delta\phi = 8.5°$). The quality of this tape was examined by depositing YBCO films using the *ex situ* BaF_2 precursor process in a reel-to-reel system. Details of this experimental procedure were reported earlier.[34,35] The results of electrical transport J_c measurements at 77 K and zero applied field, conducted over a 80 cm long section of the same YBCO/CeO_2/YSZ/Gd_2O_3/Ni tape, are shown in Fig. 12. The sectional J_c values were taken at each 1-cm increment along the tape length. The tape width is 1 cm and the thickness of the YBCO coating is 300 nm. It is clear from the figure that the sample exhibits an average J_c value of 7.5×10^5 A/cm^2 and it supports an end-to-end J_c of 6.25×10^5 A/cm^2, with some regions reaching J_c values of 1×10^6 A/cm^2. The latter value represents the best-recorded performance on short samples. The low J_c sections marked with ★ are

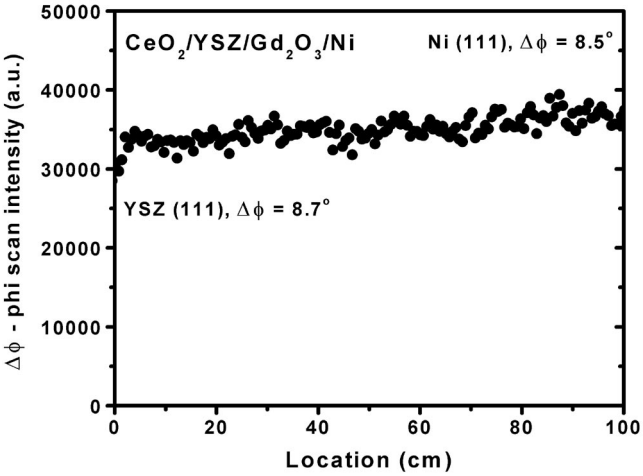

Fig. 11. Longitudinal distribution of XRD ϕ-scan intensity of YSZ(111) peak reflection for the same 1 m tape, shown in Fig. 10.

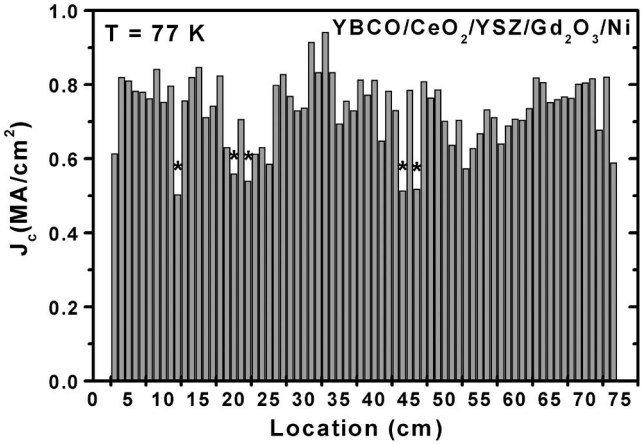

Fig. 12. Sectional J_c (77 K, self-field) values for the YBCO film obtained on 1 m long sol–gel seeded $CeO_2/YSZ/Gd_2O_3$/Ni tape. Visible line features marked by ★.

associated with visible line features along the YBCO thickness, resulting from the variations in the composition of YBCO(BaF_2) precursor films. Despite the existence of these flaws, the present results represent the first reported achievement of high-J_c YBCO performance on a long length RABiTS structure having a nonvacuum solution processed seed layer.

IV. Summary and Conclusions

We have demonstrated the fabrication of high-J_c YBCO coatings on sol–gel processed, reel-to-reel dip-coated Gd_2O_3 seed buffer layers on textured, strengthened Ni and Ni-alloy substrates, with sputtered CeO_2/YSZ overlayers. High-quality Gd_2O_3 layers were achieved at temperatures between 1100° and 1150°C under reducing forming gas (96% Ar + 4% H_2) atmosphere. It has been found that the postannealing throughput speed (S_{an}) does not have a significant affect on the in-plane alignment of Gd_2O_3. However, the out-of-plane alignment has a tendency to degrade for S_{an} exceeding 20 cm/h. Whether these findings will limit processing speeds requires further study of the independent affects of ramp rate and residence time in the furnace. The surface roughness of Gd_2O_3 films was found to depend strongly on the thickness of the layers by the combination of coating speed and solution viscosity, which produced notable differences in the growth characteristics of the subsequent YSZ and CeO_2 barrier and cap layers. The combinations of smooth morphology and crystalline cap buffer layers on thin Gd_2O_3 yielded YBCO films with self-field J_c values as high as 1.2×10^6 A/cm^2 at 77 K. The magnetic field performance of J_c was as good as that obtained for YBCO films on standard $CeO_2/YSZ/CeO_2$ buffered Ni substrates.

After establishing this proof of principle on short prototype conductors, we have presented our results on a length demonstration (100 cm) of dip-coated Gd_2O_3 seed layers on biaxially textured Ni. The YBCO films grown using the *ex situ* BaF_2 precursor approach on this nonvacuum and vacuum derived CeO_2(sputtered)/YSZ(sputtered)/Gd_2O_3(dip-coated)/Ni multilayer structure supported a mean self-field J_c value of 7.5×10^5 A/cm^2 at 77 K with some regions reaching 1×10^6 A/cm^2. These observations underscore the potential viability of nonvacuum chemical solution-based synthesis routes for the development and manufacturing of RABiTS-based coated conductors.

References

[1]A. Goyal, D. P. Norton, J. D. Budai, M. Paranthaman, E. D. Specht, D. M. Kroeger, D. K. Christen, Q. He, B. Saffian, F. A. List, D. F. Lee, P. M. Martin, C. E. Klabunde, E. Hatfield, and V. K. Sikka, "High Critical Current Density Superconducting Tapes by Epitaxial Deposition of $YBa_2Cu_3O_x$ Thick Films on Biaxially Textured Metals," *Appl. Phys. Lett.*, **69**, 1795 (1996).

[2]D. P. Norton, A. Goyal, J. D. Budai, D. K. Christen, D. M. Kroeger, E. D. Specht, Q. He, B. Saffian, M. Paranthaman, C. E. Klabunde, D. F. Lee, B. C. Sales, and F. A. List, "Epitaxial $YBa_2Cu_3O_7$ on Biaxially Textured Nickel (001): An Approach to Superconducting Tapes with High Critical Current Density," *Science (Washington D.C.)*., **274**, 755 (1996).

[3]C. M. Carlson, J. C. Price, P. A. Parilla, D. S. Ginley, D. Niles, R. D. Blaugher, A Goyal, M. Paranthaman, D. M. Kroeger, and D. K. Christen, "Laser-Ablated Epitaxial $LaAlO_3$ Buffer Layers on Biaxially Textured Ni Substrates for Superconducting Tapes," *Physica C*, **304**, 82 (1998).

[4]M. Paranthaman, D. F. Lee, A. Goyal, E. D. Specht, P. M. Martin, X. Cui, J. E. Mathis, R. Feenstra, D. K. Christen, and D. M. Kroeger, "Growth of Biaxially Textured RE_2O_3 Buffer Layers on Rolled-Ni Substrates Using Reactive Evaporation for HTS-Coated Conductors," *Supercond. Sci. Technol.*, **12**, 319 (1999).

[5]C. Cantoni, T. Aytug, D. T. Verebelyi, M. Paranthaman, E. D. Specht, D. P. Norton, and D. K. Christen, "Conductive Buffer Layers and Overlayers for the Electrical Stability of Coated Conductors," *IEEE Trans. Appl. Supercond.*, **11**, 3309 (2001).

[6]Q. He, D. K. Christen, R. Feenstra, D. P. Norton, M. Paranthaman, E. D. Specht, D. F. Lee, A. Goyal, and D. M. Kroeger, "Growth of Biaxially Oriented Conductive $LaNiO_3$ Buffer Layers on Textured Ni Tapes for High-T_c-Coated Conductors," *Physica C*, **314**, 105 (1999).

[7]T. Aytug, J. Z. Wu, C. Cantoni, D. T. Verebelyi, E. D. Specht, M. Paranthaman, D. P. Norton, D. K. Christen, R. E. Ericson, and C. L. Thomas, "Growth and Superconducting Properties of $YBa_2Cu_3O_{7-\delta}$ Films on Conductive $SrRuO_3$ and $LaNiO_3$ Multilayers for Coated Conductor Applications," *Appl. Phys. Lett.*, **76**, 760 (2000).

[8]T. Aytug, J. Z. Wu, B. W. Kang, D. T. Verebelyi, C. Cantoni, E. D. Specht, A. Goyal, and M. Paranthaman, "An All-Sputtered Buffer Layer Architecture for High-J_c $YBa_2Cu_3O_{7-\delta}$ Coated Conductors," *Physica C*, **340**, 33 (2000).

[9]T. Aytug, B. W. Kang, C. Cantoni, E. D. Specht, M. Paranthaman, A. Goyal, D. K. Christen, D. T. Verebelyi, J. Z. Wu, R. E. Ericson, C. L. Thomas, C.-Y. Yang and S. E. Babcock, "Growth and Characterization of Conductive $SrRuO_3$ and $LaNiO_3$ Multilayers on Textured Ni Tapes for High-J_c $YBa_2Cu_3O_{7-\delta}$ Coated Conductors," *J. Mater. Res.*, **16**, 2661 (2001).

[10]M. Paranthaman, A. Goyal, F. A. List, E. D. Specht, D. F. Lee, P. M. Martin, Q. He, D. K. Christen, D. P. Norton, J. D. Budai, and D. M. Kroeger, "Growth of Biaxially Textured Buffer Layers on Rolled-Ni Substrates by Electron Beam Evaporation," *Physica C*, **275**, 266 (1997).

[11]J. E. Mathis, A. Goyal, D. F. Lee, F. A. List, M. Paranthaman, D. K. Christen, E. D. Specht, D. M. Kroeger, and P. M. Martin, "Biaxially Textured Y-123 Conductors on RABiTS with Critical Current Densities of 2–3 MA/cm^2," *Jpn. J. Appl. Phys.*, **37**, L1379 (1998).

[14]C. Park, D. P. Norton, D. K. Christen, D. T. Verebelyi, R. Feenstra, J. D. Budai, A. Goyal, D. F. Lee, E. D. Specht, D. M. Kroeger, and M. Paranthaman, "Long Length Fabrication of YBCO on Rolling Assisted Biaxially Textured Substrates (RABiTS) Using Pulsed Laser Deposition," *IEEE Trans. Appl. Supercond.*, **9**, 2276 (1999).

[13]F. A. List, A. Goyal, M. Paranthaman, D. P. Norton, E. D. Specht, D. F. Lee, and D. M. Kroeger, "High J_c YBCO Films on Biaxially Textured Ni with Oxide Buffer Layers Deposited Using Electron Beam Evaporation and Sputtering," *Physica C*, **302**, 87 (1998).

[14]V. Boffa, C. Annino, D. Bettinelli, S. Ceresara, L. Ciontea, F. Fabbri, V. Galluzzi, U. Gambardella, G. Celentano, G. Grimaldi, A. Mancini, T. Petrisor, and P. Scardi, "Epitaxial growth of Heterostructures on Biaxially Textured Metallic Substrates for $YBa_2Cu_3O_{7-x}$ Tape Fabrication," *Philos. Mag. B*, **80**, 979 (2000).

[15]T. J. Jackson, B. A. Glowacki, and G. J. Schmitz, "Oxidation Thermodynamics of Metal Substrates during the Deposition of Buffer Layer Oxides," *Physica C*, **296**, 215 (1998).

[16]S. Oh, J. Yoo, K. Lee, J. Kim, and D. Youm, "Comparative Study on the Crack Formations in the CeO_2 Buffer Layers for YBCO Films on Textured Ni Tapes and Pt Tapes," *Physica C*, **308**, 91 (1998).

[17]X. Cui, F. A. List, D. M. Kroeger, A. Goyal, D. F. Lee, J. E. Mathis, E. D. Specht, P. M. Martin, R. Feenstra, D. T. Verebelyi, D. K. Christen, and M. Paranthaman, "Continuous Growth of Epitaxial CeO_2 Buffer Layers on Rolled Ni Tapes by Electron Beam Evaporation," *Physica C*, **316**, 27 (1999).

[18]E. Celik, I. H. Mutlu, and Y. S. Hascicek, "Sol–Gel Processing of Buffer Layers on Ni Tape for YBCO Surface Coated Conductors," *IEEE Trans. Appl. Supercond.*, **10**, 1162 (2000).

[19]S. Sathyamurthy and K. Salama, "Chemical Solution Deposition of Highly Oriented Strontium Titanate Buffer Layers for Coated Conductors," *Supercond. Sci. Technol.*, **13**, L1 (2000).

[20]J. C. Schmidt, A. Tiggers, and G. J. Schmitz, "Synthesis of Polycrystalline $BaZrO_3$ Coatings," *Mater. Sci. Eng., B*, **53**, 115 (1998).

[21]T. A. Gladstone, J. C. Moore, A. J. Wilkinson, and C. M. R. Grovenor, "Fabrication of Biaxially Textured Ni Substrates and $LaNiO_3$ Buffer Layers for Tl-1223 Thick Films," *IEEE Trans. Appl. Supercond.*, **9**, 2252 (1999).

[22]J. S. Morrell, Z. B. Xue, E. D. Specht, A. Goyal, P. M. Martin, D. F. Lee, R. Feenstra, D. T. Verebelyi, D. K. Christen, T. G. Chirayil, M. Paranthaman, C. E. Valet, and D. B. Beach, "Epitaxial Growth of Gadolinium Oxide on Roll-Textured Nickel Using a Solution Growth Technique," *J. Mater. Res.*, **15**, 621 (2000).

[23]M. Paranthaman, T. G. Chirayil, F. List, X. Cui, A. Goyal, D. F. Lee, E. D. Specht, P. M. Martin, R. K. Williams, D. M. Kroeger, J. S. Morrell, D. B. Beach, R. Feenstra, and D. K. Christen, "Fabrication of Long Lengths of Epitaxial Buffer Layers on Biaxially Textured Nickel Substrates Using a Continuous Reel-to-Reel Dip-Coating Unit," *J. Am. Ceram. Soc.*, **84**, 273 (2001).

[24]T. G. Chirayil, M. Paranthaman, D. B. Beach, D. F. Lee, A. Goyal, R. K. Williams, X. Cui, D. M. Kroeger, D. T. Verebelyi, and D. K. Christen, "Epitaxial Growth of $La_2Zr_2O_7$ Thin Films on Rolled-Ni Substrates by Sol–Gel Process for High T_c Superconducting Tapes," *Physica C*, **336**, 63 (2000).

[25]D. B. Beach, C. E. Valet, M. Paranthaman, E. D. Specht, J. S. Morrell, and Z. B. Xue, "Sol–Gel Synthesis of Rare Earth Aluminate Films as Buffer Layers for High T_c Superconducting Films," *Mater. Res. Soc. Symp. Proc.*, **495**, 263 (1998).

[26]M. W. Rupich, W. Palm, W. Zhang, E. Siegal, S. Annavarapu, L. Fritzemeier, M. D. Teplitsky, C. Thieme, and M. Paranthaman, "Growth and Characterization of Oxide Buffer Layers for YBCO Coated Conductors," *IEEE Trans. Appl. Supercond.*, **9**, 1527 (1999).

[27]T. G. Chirayil, M. Paranthaman, D. B. Beach, J. S. Morrell, E. Y. Sun, A. Goyal, R. K. Williams, D. F. Lee, P. M. Martin, D. M. Kroeger, R. Feenstra, D. T. Verebelyi, and D. K. Christen, "Epitaxial Growth of Yb_2O_3 Buffer Layers on Biaxially Textured-Ni (100) Substrates by Sol–Gel Process," *Mater. Res. Soc. Symp. Proc.*, **574**, 51 (1999).

[28]M. Paranthaman, T. G. Chirayil, S. Sathyamurthy, D. B. Beach, A. Goyal, F. A. List, D. F. Lee, X. Cui, S. W. Lu, B. W. Kang, E. D. Specht, P. M. Martin, D. M. Kroeger, R. Feenstra, C. Cantoni, and D. K. Christen, "Fabrication of Long Lengths of YBCO Coated Conductors Using a Continuous Reel-to-Reel Dip-Coating Unit," *IEEE Trans. Appl. Supercond.*, **11**, 3146 (2000).

[29]A. Goyal, R. Feenstra, M. Paranthaman, J. R. Thompson, B. W. Kang, C. Cantoni, D. F. Le, F. A. List, P. M. Martin, E. Lara-curio, C. Stevens, D. M. Kroeger, M. Kowalewski, E. D. Specht, T. Aytug, S. Sathyamurthy, R. K. Williams, and R. E. Ericson, "Strengthened, Biaxially Textured Ni Substrate with Small Alloying Additions for Coated Conductor Applications," *Physica C*, **382**, 251 (2002).

[30]W. Prusseit, R. Nemetschek, R. Semerad, B. Holzaphel, and J. Erickemeyer, "YBCO and Buffer Layer Deposition on Long Length Metal Tape Substrates by Thermal Evaporation"; p. 87 in Program and Extended Abstracts of the 5th International Workshop on Superconductivity Co-sponsored by ISTEC and MRS (Honolulu, HI, 2001). MRS, Boston, MA, 2001.

[31]M. Paranthaman, S. Sathyamurthy, T. Aytug, D. B. Beach, A. Goyal, B. W. Kang, R. Feenstra, D. K. Christen, D. F. Lee, P. M. Martin, L. Heatherly Jr., and D. M. Kroeger, "High Current Density YBCO Coated Conductors on Strengthened Biaxially Textured Ni–W Substrates"; p. 87 in Program and Extended Abstracts of the 5th International Workshop on Superconductivity Co-sponsored by ISTEC and MRS (Honolulu, HI, 2001). MRS, Boston, MA, 2001.

[32]H. R. Hoekstra, "Phase Relationships in the Rare Earth Sesquioxides at High Pressure," *Inorg. Chem.*, **5**, 754 (1966).

[33]M. Paranthaman, R. Feenstra, D. F. Lee, D. B. Beach, J. S. Morrell, T. G. Chirayil, A. Goyal, X. Cui, D. T. Verebelyi, J. E. Mathis, P. M. Martin, D. P. Norton, E. D. Specht, D. K. Christen, and D. M. Kroeger, "Demonstration of High Current Density YBCO Coated Conductors on RE_2O_3-Buffered Ni Substrates with Two New Alternative Architectures," *Adv. Cryog. Eng. Mater.*, **46**, 879 (2000).

[34]D. F. Lee, F. A. List, D. M. Kroeger, K. W. Childs, D. O'Neill, and W. B. Robbins, "Long-Length Conversion of Barium Fluoride Precursor Films on RABiTS"; p. 73 in Program and Extended Abstracts of the 5th International Workshop on Superconductivity Co-sponsored by ISTEC and MRS (Honolulu, HI, 2001). MRS, Boston, MA, 2001.

[35]S. W. Lu, F. A. List, D. F. Lee, X. Cui, M. Paranthaman, B. W. Kang, D. M. Kroeger, A. Goyal, P. M. Martin, and R. E. Ericson, "Electron Beam Co-evaporation of Y–BaF_2–Cu Precursor Films for $YBa_2Cu_3O_{7-\delta}$ Coated Conductors," *Supercond. Sci. Technol.*, **14**, 218 (2001). □